



Evaluation of dimerization–inhibitory activities of cyclic peptides containing a β -hairpin loop sequence of the EGF receptor

Takaaki Mizuguchi^a, Naho Ohara^a, Mika Iida^a, Ryunosuke Ninomiya^a, Shinji Wada^a, Yoshiaki Kiso^{a,†}, Kazuki Saito^{a,b}, Kenichi Akaji^{a,*}

^a Department of Medicinal Chemistry, Center for Frontier Research in Medicinal Science, Kyoto Pharmaceutical University, Kyoto 607-8412, Japan

^b Department of Integrated Biosciences, Graduate School of Frontier Sciences, University of Tokyo, Kashiwa, Chiba 277-8562, Japan

ARTICLE INFO

Article history:

Received 11 July 2012

Revised 9 August 2012

Accepted 9 August 2012

Available online 17 August 2012

Keywords:

EGF receptor

Dimerization

Inhibitor

Cyclic peptide

Retro-Inverso modification

A431 cell

ABSTRACT

Structure–activity relationships of cyclic peptides mimicking the β -hairpin structure of the ‘dimerization arm’ at residues 242–259 of the EGF receptor are examined. Cyclic peptides containing the arm head of the β -hairpin loop showed inhibitory activity toward the EGF receptor’s dimerization. Cyclic peptides containing a Retro-Inverso sequence of the dimerization arm showed clear inhibitory effects on the dimerization in vitro and efficiently suppressed the proliferation of A431 cells, which abundantly express the EGF receptor on their surface. The effects at a specific hydrophobic site of the loop structure were expected to enhance the interactions with the receptor.

© 2012 Elsevier Ltd. All rights reserved.

1. Introduction

The epidermal growth factor (EGF) receptor is a membrane-spanning protein belonging to the ErbB family (ErbB1–4).^{1,2} The receptor is closely involved in cell proliferation and differentiation, and its overexpression or unregulated activation can lead to the aberrant growth of cancer cells such as non-small cell lung cancer (NSCLC) cells.^{3–6} Thus, it is a target of anti-cancer drugs such as gefitinib (Iressa[®]) which directly inhibits its intracellular tyrosine kinase domain.^{7,8} Antibodies against the EGF receptor also have been developed as anti-cancer agents; cetuximab (Erbbitux[®]), for example, is a monoclonal antibody recognizing the extracellular ligand-binding region of the receptor.^{9–11} Although these agents are effective as cancer therapeutics, their use has several drawbacks including side effects¹² and exorbitant costs.^{13,14} A new type of inhibitor against the EGF receptor is eagerly anticipated for improving the quality of life of cancer patients.

Activation of the EGF receptor is triggered by the binding of EGF to the extracellular region followed by a conformational change causing the receptor’s dimerization.¹⁵ The dimerization induces intracellular autophosphorylation, in which a kinase domain of each

receptor *trans*-phosphorylates the tyrosine residue at the C-terminal tail of the partner.^{16–18} The phosphorylation induces cell growth through activation of an intracellular signaling pathway.^{19,20}

The extracellular structure of the dimerized EGF receptor has been elucidated by X-ray crystallographic studies (PDB ID: 1IVO).²¹ The receptor’s extracellular region consists of four domains (I–IV), with most of the interface region of the dimer composed of domain II. A β -hairpin arm at residues 242–259 in domain II is thought to be essential to maintaining the dimeric structure (Fig. 1).²¹ Tyr246, Thr249, Tyr251, and Gln252 of the β -hairpin arm form hydrogen bonds with Cys283, Asn86, Arg285, and Ala286 of the counterpart, respectively, to tightly hold together the active dimer. Thus, the β -hairpin structure is known as the ‘dimerization arm’, and is expected to exist in all ErbB receptors (ErbB-1–4) including homo- and hetero-dimer receptors.^{22–25}

Because of the key function of the ‘dimerization arm’ to hold together the receptor, peptide sequences of the arm have been used as a template to design novel compounds with inhibitory activity toward the functional dimer. Several compounds such as Inherbin3²⁶ and NSC56452²⁷ derived from the arm structure have been reported. We also have developed a cyclic decapeptide (**1**, CYNPTTYQMC) which mimics the loop structure of the arm, and showed that it inhibits the dimerization of the EGF receptor.²⁸ In the present study, we examined the structure–activity relationships of **1** in detail focusing on (i) the ring’s size by adding or removing the corresponding amino acids of the arm, (ii) the ring’s

* Corresponding author. Tel.: +81 75 595 4636; fax: +81 75 591 9900.

E-mail address: akaji@mb.kyoto-phu.ac.jp (K. Akaji).

† Present address: Department of BioScience, Nagahama Institute of Bio-Science and Technology, Tamura-cho, Nagahama, Shiga 526-0829, Japan.

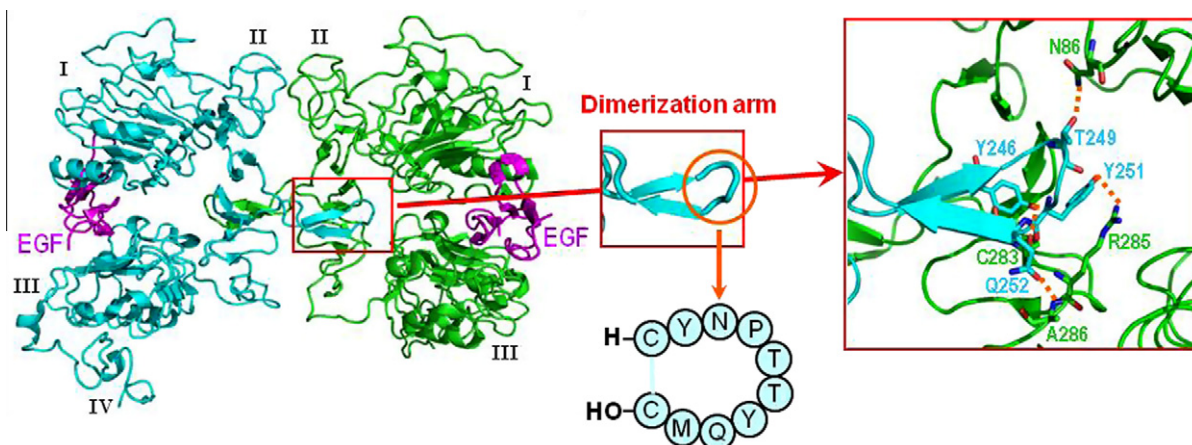


Figure 1. Structure of the EGF receptor dimer (left) and the intermolecular hydrogen-bonds at the dimerization arm (right inset) (PDB ID: 1IVO). The extracellular region of the receptor consists of four domains (I–IV) with the interface mostly occupied by domain II. Four representative hydrogen-bonds between Tyr246^A and Cys283^B, Thr249^A and Asn86^B, Tyr251^A and Arg285^B, and Gln252^A and Ala286^B are shown in the inset (A and B at each residue indicate monomer A in blue and monomer B in green).

position by shifting two cysteine residues, (iii) the effect of adding an extra sequence to the ring by elongating amino acids at the N- or C-terminus, and (iv) the topology of the side-chain structure by inverting the sequence and/or stereo-structure. The inhibitory activity for receptor dimerization was assessed using membrane extracts from human epidermal carcinoma A431 cells, which abundantly express the EGF receptor on their surface.²⁹

2. Results and discussion

2.1. Effects of the ring structure

To evaluate the effect of ring-size on the dimerization's inhibition, twelve peptides (**2–13**) were designed (Fig. 2 A). Since most of these peptides have Tyr246, Thr249, Tyr251, and Gln252 supposed to be key residues in the β -hairpin arm structure, examining their effects on receptor dimerization would provide insight into

the role of the ring structure. Peptides **2–4** having a fairly large ring are expected to have a loop with a β -hairpin-like structure, since each disulfide bond is replaced at a site where the bond distance is similar to that of the corresponding β -hairpin site determined by X-ray crystallographic studies.²¹ Peptides **5–7** have a slightly larger ring than **1**; the differences are in the range of 1–2 amino acids residues. Peptides **8** and **9** have a slightly smaller ring than **1** due to the removal of one or two residues. Peptides **10–12** also have a smaller ring than **1** caused by a shift in the position of the cysteine residue toward the inside of the ring structure to make the ring more compact. **13** contains two disulfide bonds, a combination of **1** and **12**, which would make the ring structure more rigid.

The test peptides were produced by conventional Fmoc-based solid-phase peptide synthesis using 2-chlorotrityl resin. Single disulfide bonds were constructed by air-oxidation without difficulty, and double disulfide bonds by successive oxidation with air and iodine. To avoid the conversion of Met to Met(O) by iodine, the second oxidation reaction by iodine was stopped within a minute. The homogeneity of each peptide was confirmed by analytical HPLC and high-resolution FAB-MS. Dimerization-inhibitory activities of the synthetic peptides were assessed using membrane extracts of A431 cells, according to published procedures^{28,30} with minor modifications. Briefly, the ligand-induced dimer receptor was covalently linked by a hydrophilic, membrane-impermeable cross-linker, bis (sulfosuccinimidyl) suberate (BS³).³¹ The monomer (~170 kDa) and dimer (~350 kDa) of the receptor were separated by SDS-PAGE and detected by immuno-blotting with an anti-EGFR antibody. The amount of monomer and dimer was quantified by densitometry of the bands (Fig. S3). The inhibitory activity of 10 μ M of **1** was used as a reference standard in each assay.

Amounts of the dimeric receptor in the presence of test peptides are summarized in Figure 2 B in which the amount without any peptide is taken as 1.0. As previously reported,²⁸ **1** decreased the amount of the dimer by inhibiting its formation; 10 μ M of **1** reduced the amount to 69% of the control. The amounts of dimer in the presence of **2–4** having a large ring were similar to the amount obtained with **1**, and in the presence of peptides **5–7** having a slightly large ring, a little higher (~80%). The results suggest that the peptides with a fairly large ring have the flexibility to adjust their structure similar to that of the dimerization arm to show inhibitory activity toward the dimer's formation, whereas a slightly large ring would have rigidity to hold the arm in a somewhat different structure.

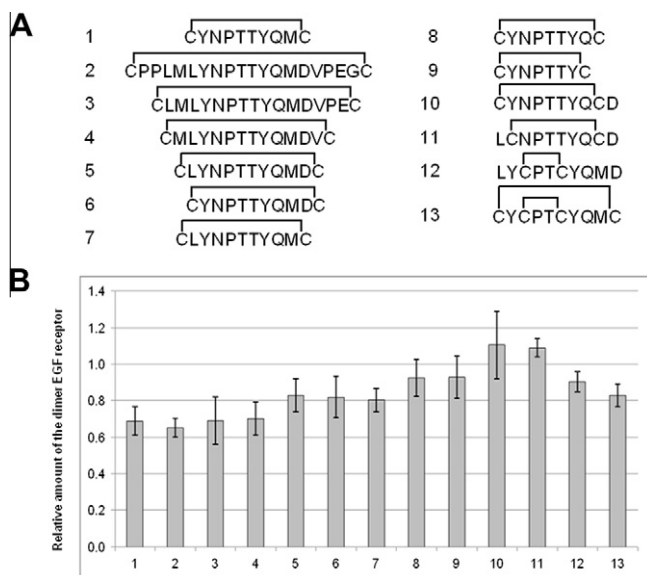


Figure 2. (A) Structure of the synthesized cyclic peptides (**1–13**). (B) Amounts of the receptor dimer in the presence of the cyclic peptides. The amount of the dimer without the peptide is taken as 1.0. The results are shown as the mean \pm standard deviation for at least three independent experiments performed in duplicate.

In contrast, peptides **8–12** with a smaller ring had little effect on the receptor's dimerization, which suggests that the small ring has a major effect on the side-chain orientation necessary to maintain the arm's structure. **12** decreased the amount of the dimer to 90%, which indicates that 32% of the inhibitory activity of **1** was recovered (a 10% decrease in **12** vs 31% decrease in **1**). The double cyclized peptide **13** showed more effective inhibitory activity; the amount of dimer was reduced to 83%, indicating 65% of the inhibitory activity of **1** was recovered (a 20% decrease in **13** vs 31% decrease in **1**). The positions of two cysteine residues of **12** correspond to Asn247 and Thr250 of the dimerization arm. According to crystallographic studies (Fig. 1), these two residues occupy an arm head region in the dimerization interactions and a hydrogen bond is estimated to exist between the side-chains. Thus, the specific small ring which can hold the arm head structure might compensate for the negative effects due to the downsizing of the ring structure to recover the minimum interactions necessary for the dimer to form. The rigid structure of the double disulfide of **13** might work more effectively than **12** to maintain the necessary arm head structure resulting in an increase in inhibitory activity. Taken together, the results summarized in Figure 2 suggest that the loop structure of the β -hairpin arm, especially its arm head, is critical for the receptor dimerization induced by EGF-binding, and thus, peptide mimics of this arm would have inhibitory effects on the dimerization.

2.2. Effects of additional sequences in the ring structure

To evaluate the effects of adding amino acid residues to the core arm structure, **14–19** were synthesized (Fig. 3). Peptides **14–16** have an additional N-terminal sequence of the β -hairpin loop and **17–19** have an additional C-terminal sequence. As shown in Figure 3 B, **14** having an extra Met residue reduced the amount of dimer slightly more than **1** (64% vs 69%), that is, the inhibitory activity of **14** was slightly increased. Further addition to the N-terminus, however, decreased the inhibitory effect as in **15** and **16**. Adding

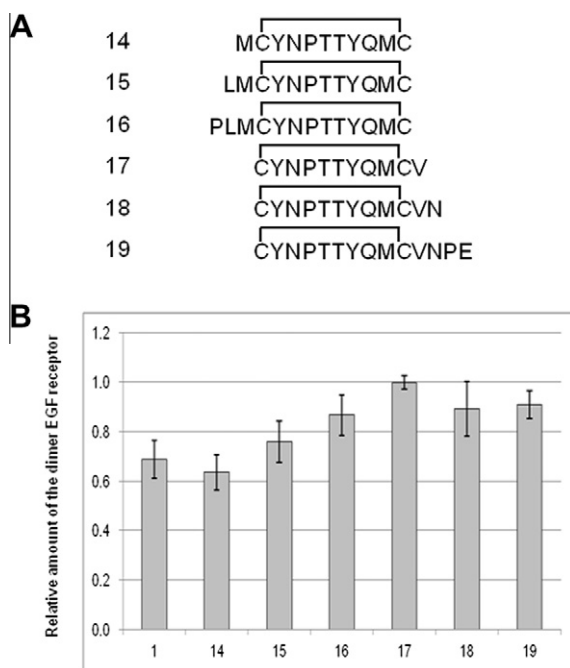


Figure 3. (A) Structure of the synthesized cyclic peptides (**14–19**). (B) Amounts of the receptor dimer in the presence of the cyclic peptides. The amount of the dimer without the peptide is taken as 1.0. The results are shown as the mean \pm standard deviation for at least three independent experiments performed in duplicate.

amino acids to the C-terminus abolished the inhibitory activity (peptides **17–19**). Thus, the addition of residues to the β -hairpin structure had little effect on the inhibitory activity of the arm mimics. These results suggest that the β -hairpin structure of **1** interacts closely with the dimer counterpart and the addition of amino acid residues to the ring structure hinders the interaction probably due to steric effects. Based on these results, the effects of the side-chain topology of **1**, both overall and at specific residues, were then examined.

2.3. Effects of the side-chain structure

To evaluate the overall side-chain topology, a Retro-Inverso (RI) form of **1**, the peptide **20**, was synthesized. This modification involves a reversion of the peptide sequence accompanied by the replacement of each L-amino acid with the corresponding D-amino acid. RI-modified biologically active peptides have been found to retain the recognition properties or biological activities of the parent peptides, since a similar topography of side chain orientations can be maintained.^{32,33} Similar or improved interactions of RI-modified peptides with proteins or receptors have also been reported.^{34,35} In addition, the introduction of D-amino acids enhances resistance to enzymatic degradation.³⁶

For comparison, **21** modified only by a reversion of the original sequence with L-amino acids and **22** having the original sequence of D-amino acids were also synthesized. As summarized in Figure 4, nearly the same amount (68%) of dimer was detected in the presence of the RI-modified peptide **20**, which indicates that **20** has the same inhibitory activity as **1**. In contrast, **21** and **22** had little effect on the receptor's dimerization. These results strongly suggest that the overall topology of the side-chains of **1** is critical to the interactions at the dimerization arm.

The effects of substitutions at a specific residue were then examined focusing on neighboring positions of the ring structure of **1**, since a shift of the disulfide positions inside the ring completely abolished the inhibitory activity (Fig. 2 **10** and **11**). Thus, **23** having Ala instead of Tyr246, a C-terminal residue next to Cys245 in **1**, and **24–28** having substitutions at Met253, an

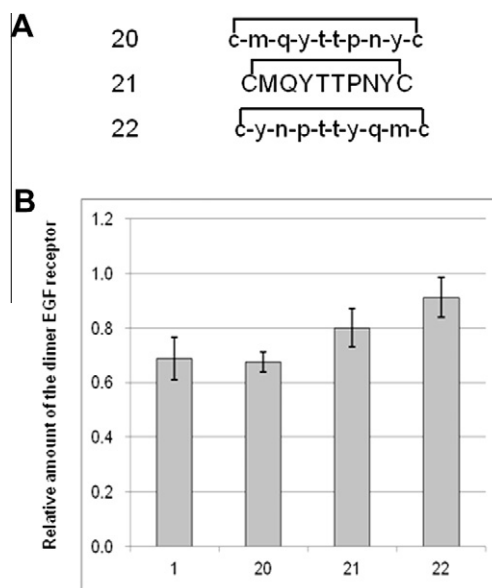


Figure 4. Structure of the synthesized cyclic peptides (**20–22**). Small characters in the sequence indicate D-amino acids. (B) Amounts of the receptor dimer in the presence of the cyclic peptides. The amount without the peptide is taken as 1.0. The results are shown as the mean \pm standard deviation for at least three independent experiments performed in duplicate.

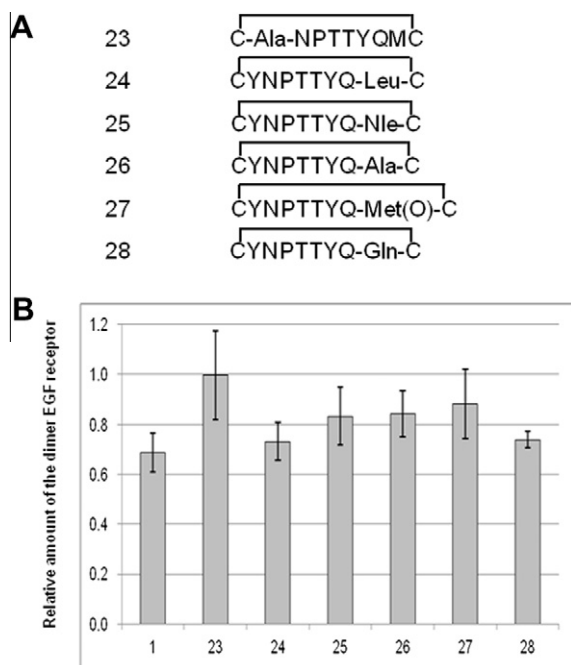


Figure 5. (A) Structure of the synthesized cyclic peptides (23–28). (B) Amounts of the receptor dimer in the presence of the cyclic peptides. The amount without the peptide is taken as 1.0. The results are shown as the mean \pm standard deviation for at least three independent experiments performed in duplicate.

N-terminal residue next to Cys254, were synthesized. Peptides **24–26** had a non-polar aliphatic side-chain structure (Leu, Nle, and Ala, respectively) and **27** and **28**, a polar neutral side-chain structure (Met(O) and Gln).

The substitution of Tyr246 in **23** completely abolished the inhibitory activity (Fig. 5) probably due to the loss of the hydrogen bond at this site (see Fig. 1). In contrast, peptides substituted at position 253 decreased the amount of dimer in the range of 73–88%, which indicates that the substitutions at this site maintained the inhibitory activity. Notably, the γ -branched structure (Leu) and planer amide structure (Gln) having nearly the same size as Met maintained the inhibitory activity, while the short (Ala) or long aliphatic side-chain (Nle) and polar sulfoxide (Met(O)) structures lowered or almost abolished the activity. The results suggest that some hydrophobic area remained unoccupied at this site, which would agree with previous X-ray crystallographic studies on the EGF receptor's interaction with TGF α indicating that Met253 of the dimerization arm participates in the hydrophobic interaction in the complex.³⁷

2.4. Inhibitory effects on EGF receptor autophosphorylation

The inhibitory effect of the RI-modified peptide **20** on autophosphorylation of the receptor was then evaluated using the intact A431 cells. For comparison, the effect of **1** was also examined in parallel. The cell-based assay was performed by immunoblotting as described previously²⁸ with minor modifications. In this assay, an anti-EGFR [pY1068] ABfinity™ antibody, which specifically recognizes the receptor phosphorylated at Tyr1068, was used as a primary antibody. Tyr1068 at the C-terminal tail of the intracellular domain is an autophosphorylation site that allows binding of Grb2 and activation of the Ras-Raf-ERK1/ERK2 signaling pathway, which is deeply related to the cell proliferation and differentiation.³⁸

In the presence of **20**, autophosphorylation of the receptor was decreased by approximately 45% at the concentration of 1 nM and

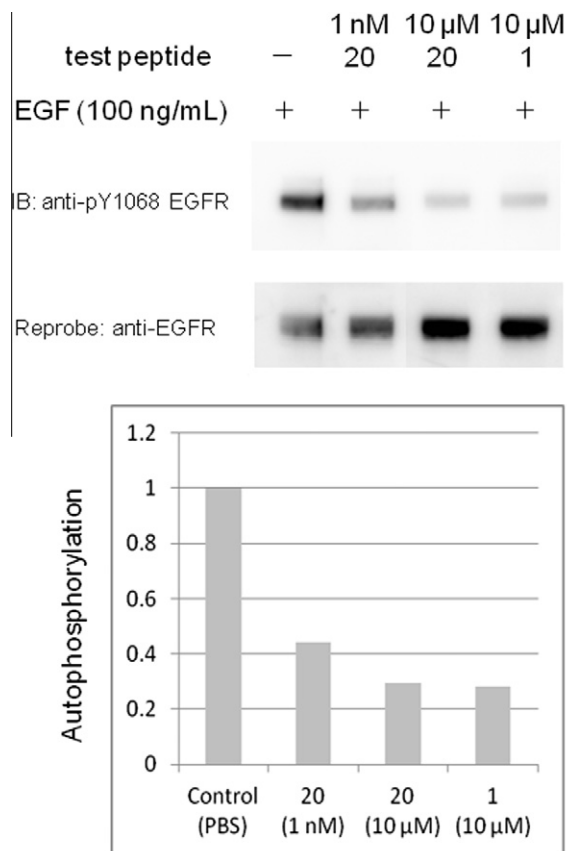


Figure 6. (A) Typical immunoblotting bands of the autophosphorylated EGF receptor. (B) Inhibitory effects of the peptide **20** on the autophosphorylation. EGF-stimulated autophosphorylation in the absence of the test peptide is taken as 1.0. Data represent the mean for two independent experiments performed in duplicate.

70% at 10 μ M (Fig. 6). The parent peptide **1** showed nearly the same inhibitory effect at 10 μ M as previously reported.²⁸ The results suggest that **20** suppresses the EGF-stimulated intracellular autophosphorylation in living cells dose dependently, and would have an inhibitory effect on cell proliferation.

2.5. Inhibitory effects on cell proliferation

To estimate the effect in vivo, the inhibitory activity of the RI-modified peptide **20** in A431 cells was evaluated. For comparison, that of **1** and Inherbin3, an inhibitory peptide of the EGF receptor reported by Xu et al.²⁶ was also examined. As shown in Figure 7 **20** suppressed cell proliferation to 81% of that with vehicle (distilled water), more than did the parent peptide **1** (84%) and Inherbin3 (95%). Thus, the peptide **20** suppresses the dimer's formation and autophosphorylation, which leads to a reduction in cell growth. The results can be explained in terms of the metabolic stability of the RI-modified peptide as well as its arm mimic.

3. Conclusion

Peptides containing a β -hairpin loop structure at residues 242–259 of the EGF receptor can mimic a key function of the 'dimerization arm' to fold the dimeric structure induced by EGF-binding, and peptide mimics of this arm have inhibitory effects on the dimerization. An arm head structure of the β -hairpin loop was found to be critical for the receptor's dimerization, since peptide mimics of this small arm head showed inhibitory effects on the dimerization. The

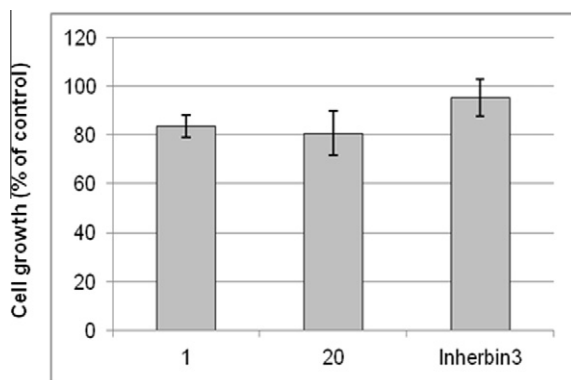


Figure 7. Inhibition of A431 cell proliferation. A431 cells were seeded in DMEM (containing 10% FBS and antibiotics) and treated with **1**, **20**, and Inherbin3. Cell growth with distilled water instead of the peptide was used as a 100% cell growth control. Data represent the mean \pm standard deviation for three independent experiments performed in triplicate.

RI-modified peptide showed a similar level of inhibitory activity to the parent peptide **1** in vitro and suppressed the proliferation of A431 cells more effectively than **1**, which strongly suggests that the overall topology of the side-chains plays an important role in the interactions of the arm mimics with the receptor. The side-chain structure at Met253 might be a specific hydrophobic site that enhances interaction with the receptor. Further modifications focusing on the side-chain interactions are currently underway in our laboratory.

4. Experimental

4.1. General

The Fmoc amino acid derivatives, Asp(t-Bu), Glu(t-Bu), Thr(t-Bu), Tyr(t-Bu), Lys(Boc), Trp(Boc), Cys(Trt), Cys(Acm), Asn(Trt), and Gln(Trt), were purchased from Calbiochem-Novabiochem Japan Ltd. (Tokyo, Japan) or Watanabe Chemical Ind., Ltd (Hiroshima, Japan). The human epidermal carcinoma A431 cells were from American Type Culture Collection (ATCC; Manassas, VA), and fetal bovine serum (FBS) from Thermo Fisher Scientific Inc. (Rockford, IL). The reagents were purchased from Nacali Tesque (Kyoto, Japan) and used without further purification.

Analytical HPLC was performed using a C18 reversed phase column (4.6 \times 150 mm; YMC Pack ODS AM) at 40 $^{\circ}$ C with a binary solvent system; a linear gradient of CH₃CN in 0.1% aqueous TFA at a flow rate of 0.9 mL/min with detection at 230 nm. Preparative HPLC was carried out using a C18 reversed phase column (20 \times 250 mm; YMC Pack ODS AM) at 40 $^{\circ}$ C with a binary solvent system; a linear gradient of CH₃CN in 0.1% aqueous TFA at a flow rate of 5 mL/min with detection at 230 nm. The solvents were of HPLC grade. MALDI-TOF-MS spectra were recorded on a Voyager DE-STR using α -cyano-4-hydroxy cinnamic acid as a matrix. High resolution FAB-MS spectra were obtained on a JEOL JMS-SX102A spectrometer.

4.2. Cys-Tyr-Asn-Pro-Thr-Thr-Tyr-Gln-Cys **8**

First, 400 mg (0.52 mmol) of 2-chlorotriptyl chloride resin (1.3 mmol/g) was agitated in CH₂Cl₂ (3.0 mL) at 25 $^{\circ}$ C for 10 min. Next, Fmoc-Cys(Trt)-OH (150 mg, 0.26 mmol) and diisopropylethylamine (DIPEA) (91 μ L, 0.52 mmol) were added and the mixture was stirred for 150 min at 25 $^{\circ}$ C. The resin was washed with DMF, CHCl₃, and MeOH, and dried in vacuo. To the resulting resin

(150 mg, 0.050 mmol) were added 2% (v/v) 1,8-diazabicyclo[5.4.0]undec-7-ene (DBU) and 2% (v/v) piperidine in DMF (1.0 mL) and the mixture was stirred for 5 min at 25 $^{\circ}$ C then washed with DMF (5 \times) and CHCl₃ (2 \times). Fmoc-Gln(Trt)-OH (74 mg, 0.12 mmol), 1-hydroxybenzotriazole (HOBt) (19 mg, 0.12 mmol), TBTU (2-(1*H*-benzotriazol-1-yl)-1,1,3,3-tetramethyluronium tetrafluoroborate) (39 mg, 0.12 mmol), and DIPEA (42 μ L, 0.24 mmol) in DMF (2.0 mL) were added, the mixture was stirred for 1 h at 25 $^{\circ}$ C, and the resin was washed with DMF (5 \times). Successive condensation of the corresponding Fmoc amino acid derivatives was carried out by repeating the same deprotection/coupling protocol. The N-terminal Fmoc-Cys(Trt)-OH (71 mg, 0.12 mmol) was condensed using DIC (diisopropylcarbodiimide) (19 μ L, 0.12 mmol) and HOBt (19 mg, 0.12 mmol) in DMF (2.0 mL) at 25 $^{\circ}$ C for 1 h. The protected peptide-resin (84 mg) was treated with trifluoroacetic acid (TFA)-ethanedithiol-triisopropylsilane-H₂O (94.5:2.5:1:2.5, 2.0 mL) at 25 $^{\circ}$ C for 90 min. The mixture was filtered and the filtrate was concentrated in vacuo. Cold diethyl ether (30 mL) was added to the residue. The product was suspended in distilled H₂O and lyophilized to give 19 mg (27%) of crude product. HPLC retention time (rt), 22.96 min [YMC-Pack ODS-AM (4.6 \times 150 mm), 0.9 ml/min, CH₃CN (0–100%)/100 min], MALDI-TOF-MS; found 1114.1617 for [M+Na]⁺, calcd 1114.3950 for C₄₆H₆₅N₁₁O₁₆S₂Na.

The crude peptide (12 mg) in an ammonium bicarbonate buffer (120 mL, pH 8.1, peptide concentration of 0.1 mg/mL) was stirred in air at 25 $^{\circ}$ C. An aliquot (50 μ L) was subjected to analytical reversed-phase HPLC [YMC-Pack ODS-AM (4.6 \times 150 mm), 40 $^{\circ}$ C, 0.1% TFA/CH₃CN (0–100%)/100 min] in H₂O, 0.9 ml/min]. After 10 h, the solution was lyophilized to yield a white powder containing ammonium bicarbonate (70 mg): MALDI-TOF-MS; found 1112.3088 for [M+Na]⁺, calcd 1112.3793 for C₄₆H₆₃N₁₁O₁₆S₂Na. The product was purified by preparative RP-HPLC [YMC-Pack ODS-AM (20 \times 250 mm), 40 $^{\circ}$ C, 0.1% TFA/CH₃CN (15–55%)/80 min] in H₂O, 5 ml/min]. Yield 2.3 mg (19%). HPLC rt, 18.91 min (single peak) [YMC-Pack ODS-AM (4.6 \times 150 mm), 0.9 ml/min, CH₃CN (0–50%)/50 min], FAB-MS; found 1112.3800 for [M+Na]⁺, calcd. 1112.3793 for C₄₆H₆₃N₁₁O₁₆S₂Na.

Other cyclic peptides containing a single disulfide bond were similarly synthesized and purified. All test compounds showed \geq 95% purity (Fig. S2).

peptide 2

HPLC rt, 35.00 min (single peak) [YMC-Pack ODS-AM (4.6 \times 150 mm), 0.9 ml/min, CH₃CN (0–50%)/50 min, (50–100%)/5 min], FAB-MS; found 2405.9902 for [M+Na]⁺, calcd. 2405.9891 for C₁₀₃H₁₅₄N₂₄O₃₃S₄Na.

peptide 3

HPLC rt, 33.28 min (single peak) [YMC-Pack ODS-AM (4.6 \times 150 mm), 0.9 ml/min, CH₃CN (0–50%)/50 min], FAB-MS; found 2154.8613 for [M+Na]⁺, calcd. 2154.8621 for C₉₁H₁₃₇N₂₁O₃₀S₄Na.

peptide 4

HPLC rt, 31.00 min (single peak) [YMC-Pack ODS-AM (4.6 \times 150 mm), 0.9 ml/min, CH₃CN (0–50%)/50 min], FAB-MS; found 1701.6405 for [M+Na]⁺, calcd. 1701.6397 for C₇₁H₁₀₆N₁₆O₂₃S₄Na.

peptide 5

HPLC rt, 26.53 min (single peak) [YMC-Pack ODS-AM (4.6 \times 150 mm), 0.9 ml/min, CH₃CN (0–50%)/50 min], FAB-MS; found 1471.5305 for [M+Na]⁺, calcd. 1471.5308 for C₆₁H₈₈N₁₄O₂₁S₃Na.

peptide 6

HPLC rt, 22.41 min (single peak) [YMC-Pack ODS-AM (4.6 × 150 mm), 0.9 ml/min, CH₃CN (0–50%)/50 min], FAB-MS; found 1358.4464 for [M+Na]⁺, calcd. 1358.4468 for C₅₅H₇₇N₁₃O₂₀S₃Na.

peptide 7

HPLC rt, 27.18 min (single peak) [YMC-Pack ODS-AM (4.6 × 150 mm), 0.9 ml/min, CH₃CN (0–50%)/50 min], FAB-MS; found 1356.5045 for [M+Na]⁺, calcd. 1356.5039 for C₅₇H₈₃N₁₃O₁₈S₃Na.

peptide 9

HPLC rt, 20.31 min (single peak) [YMC-Pack ODS-AM (4.6 × 150 mm), 0.9 ml/min, CH₃CN (0–50%)/50 min], FAB-MS; found 984.3202 for [M+Na]⁺, calcd. 984.3208 for C₄₁H₅₅N₉O₁₄S₂Na.

peptide 10

HPLC rt, 19.21 min (single peak) [YMC-Pack ODS-AM (4.6 × 150 mm), 0.9 ml/min, CH₃CN (0–50%)/50 min], FAB-MS; found 1227.4059 for [M+Na]⁺, calcd. 1227.4063 for C₅₀H₆₈N₁₂O₁₉S₂Na.

peptide 11

HPLC rt, 21.25 min (single peak) [YMC-Pack ODS-AM (4.6 × 150 mm), 0.9 ml/min, CH₃CN (0–50%)/50 min], FAB-MS; found 1177.4274 for [M+Na]⁺, calcd. 1177.4270 for C₄₇H₇₀N₁₂O₁₈S₂Na.

peptide 12

HPLC rt, 25.27 min (single peak) [YMC-Pack ODS-AM (4.6 × 150 mm), 0.9 ml/min, CH₃CN (0–50%)/50 min], FAB-MS; found 1256.4397 for [M+Na]⁺, calcd. 1256.4402 for C₅₃H₇₅N₁₁O₁₇S₃Na.

peptide 14

HPLC rt, 25.75 min (single peak) [YMC-Pack ODS-AM (4.6 × 150 mm), 0.9 ml/min, CH₃CN (0–50%)/50 min], FAB-MS; found 1374.4609 for [M+Na]⁺, calcd. 1374.4603 for C₅₆H₈₁N₁₃O₁₈S₄Na.

peptide 15

HPLC rt, 28.22 min (single peak) [YMC-Pack ODS-AM (4.6 × 150 mm), 0.9 ml/min, CH₃CN (0–50%)/50 min], FAB-MS; found 1487.5441 for [M+Na]⁺, calcd. 1487.5444 for C₆₂H₉₂N₁₄O₁₉S₄Na.

peptide 16

HPLC rt, 30.65 min (single peak) [YMC-Pack ODS-AM (4.6 × 150 mm), 0.9 ml/min, CH₃CN (0–50%)/50 min], FAB-MS; found 1584.5978 for [M+Na]⁺, calcd. 1584.5971 for C₆₇H₉₉N₁₅O₂₀S₄Na.

peptide 17

HPLC rt, 27.15 min (single peak) [YMC-Pack ODS-AM (4.6 × 150 mm), 0.9 ml/min, CH₃CN (0–50%)/50 min], FAB-MS; found 1342.4875 for [M+Na]⁺, calcd. 1342.4882 for C₅₆H₈₁N₁₃O₁₈S₃Na.

peptide 18

HPLC rt, 24.75 min (single peak) [YMC-Pack ODS-AM (4.6 × 150 mm), 0.9 ml/min, CH₃CN (0–50%)/50 min], FAB-MS; found 1456.5309 for [M+Na]⁺, calcd. 1456.5312 for C₆₀H₈₇N₁₅O₂₀S₃Na.

peptide 19

HPLC rt, 25.33 min (single peak) [YMC-Pack ODS-AM (4.6 × 150 mm), 0.9 ml/min, CH₃CN (0–50%)/50 min], FAB-MS; found 1682.6271 for [M+Na]⁺, calcd. 1682.6265 for C₇₀H₁₀₁N₁₇O₂₄S₃Na.

peptide 20

HPLC rt, 21.80 min (single peak) [YMC-Pack ODS-AM (4.6 × 150 mm), 0.9 ml/min, CH₃CN (0–50%)/50 min], FAB-MS; found 1243.4202 for [M+Na]⁺, calcd. 1243.4198 for C₅₁H₇₂N₁₂O₁₇S₃Na.

peptide 21

HPLC rt, 21.59 min (single peak) [YMC-Pack ODS-AM (4.6 × 150 mm), 0.9 ml/min, CH₃CN (0–50%)/50 min], FAB-MS; found 1243.4203 for [M+Na]⁺, calcd. 1243.4198 for C₅₁H₇₂N₁₂O₁₇S₃Na.

peptide 22

HPLC rt, 22.31 min (single peak) [YMC-Pack ODS-AM (4.6 × 150 mm), 0.9 ml/min, CH₃CN (0–50%)/50 min], FAB-MS; found 1243.4196 for [M+Na]⁺, calcd. 1243.4198 for C₅₁H₇₂N₁₂O₁₇S₃Na.

peptide 23

HPLC rt, 20.22 min (single peak) [YMC-Pack ODS-AM (4.6 × 150 mm), 0.9 ml/min, CH₃CN (0–50%)/50 min], FAB-MS; found 1151.3933 for [M+Na]⁺, calcd. 1151.3936 for C₄₅H₆₈N₁₂O₁₆S₃Na.

peptide 24

HPLC rt, 24.85 min (single peak) [YMC-Pack ODS-AM (4.6 × 150 mm), 0.9 ml/min, CH₃CN (0–50%)/50 min], FAB-MS; found 1225.4641 for [M+Na]⁺, calcd. 1225.4634 for C₅₂H₇₄N₁₂O₁₇S₂Na.

peptide 25

HPLC rt, 24.97 min (single peak) [YMC-Pack ODS-AM (4.6 × 150 mm), 0.9 ml/min, CH₃CN (0–50%)/50 min], FAB-MS; found 1225.4637 for [M+Na]⁺, calcd. 1225.4634 for C₅₂H₇₄N₁₂O₁₇S₂Na.

peptide 26

HPLC rt, 19.14 min (single peak) [YMC-Pack ODS-AM (4.6 × 150 mm), 0.9 ml/min, CH₃CN (0–50%)/50 min], FAB-MS; found 1183.4166 for [M+Na]⁺, calcd. 1183.4165 for C₄₉H₆₈N₁₂O₁₇S₂Na.

peptide 27

HPLC rt, 19.40 min (single peak) [YMC-Pack ODS-AM (4.6 × 150 mm), 0.9 ml/min, CH₃CN (0–50%)/50 min], FAB-MS; found 1259.4143 for [M+Na]⁺, calcd. 1259.4147 for C₅₁H₇₂N₁₂O₁₈S₃Na.

peptide 28

HPLC rt, 19.28 min (single peak) [YMC-Pack ODS-AM (4.6 × 150 mm), 0.9 ml/min, CH₃CN (0–50%)/50 min], FAB-MS; found 1240.4377 for [M+Na]⁺, calcd. 1240.4379 for C₅₁H₇₁N₁₃O₁₈S₂Na.

4.2.26. H-Leu-Val-Tyr-Asn-Lys-Leu-Thr-Phe-Gln-Leu-Glu-Pro-Asn-Pro-His-Thr-Lys-OH (Inherbin3)

HPLC rt, 28.37 min (single peak) [YMC-Pack ODS-AM (4.6 × 150 mm), 0.9 ml/min, CH₃CN (0–50%)/50 min], FAB-MS;

found 2064.0891 for $[M+Na]^+$, calcd. 2064.0894 for $C_{95}H_{148}N_{24}O_{26}Na$.

4.3. **13**

H-Cys-Tyr-Cys(Acm)-Pro-Thr-Cys(Acm)-Tyr-Gln-Met-Cys-OH **13'** was synthesized as described above. A solution of the crude peptide **13'** (11 mg) in an ammonium bicarbonate buffer (50 mL, pH 8.0) was stirred in air at 25 °C, and the reaction was monitored as above. After 47 h, the solution was lyophilized to yield 10 mg (91%) of a cyclized peptide **13'**: MALDI-TOF MS; found 1376.24 for $[M+Na]^+$, calcd 1376.45 for $C_{55}H_{79}N_{13}O_{17}S_5Na$. The obtained peptide **13'** (3.1 mg) was mixed with 0.1 M I_2 in 50% AcOH (2.5 mL, 100 equiv) and the solution was stirred for 1 min at 25 °C. Two drops of 1 M ascorbic acid solution in H_2O were added and the solution was concentrated in vacuo. The product was purified by preparative RP-HPLC as above to yield 0.36 mg (12%) of **13** as a white amorphous powder: HPLC rt, 25.13 min (single peak) [YMC-Pack ODS-AM (4.6 × 150 mm), 0.9 ml/min, CH_3CN (0–50%)/50 min], FAB-MS; found 1232.3312 for $[M+Na]^+$, calcd. 1232.3319 for $C_{49}H_{67}N_{11}O_{15}S_5Na$.

4.4. Inhibition assay for EGF receptor dimerization

A431 cells were cultured in Dulbecco's modified Eagle's medium containing 4.5 g/L glucose, L-glutamine, and sodium pyruvate (DMEM) supplemented with 10% fetal bovine serum (FBS) and 1% penicillin–streptomycin (v/v; 10,000 units/mL and 10,000 µg/mL, respectively) at 37 °C under a humidified atmosphere of 5% CO_2 . The cells (confluent in a 10-cm dish) were washed five times with PBS, collected with a cell scraper, and centrifuged at $2300 \times g$ at 4 °C for 5 min. The pellets were solubilized for 10 min with 1 ml of a buffer containing 20 mM HEPES (pH 7.4), 1% (v/v) Triton X-100, 10% (v/v) glycerol, 1 mM EGTA, and 1 mM phenylmethylsulfonyl fluoride (PMSF). The extract was centrifuged at $250,000 \times g$ for 10 min at 4 °C, and the protein concentration of the supernatant was determined with a BCA™ Protein Assay kit (Thermo Fisher Scientific Inc.). An aliquot of the supernatant, diluted with the solubilization buffer to 2 µg/µL protein, was pre-treated with 10 µM of each test peptide for 60 min. After incubation with or without 1.4 µg/mL (0.21 µM) of human EGF (recombinant, R&D Systems, Inc., Minneapolis, MN, USA) for 10 min, the mixture was treated with 1 mM BS^3 (Thermo Fisher Scientific Inc.) for 10 min. Next, 50 mM of glycine was added to terminate the cross-linking reaction. Dithiothreitol (DTT) and Novex® Tris-Glycine SDS sample buffer (2×) (Life Technologies Corporation, Carlsbad, CA, USA) were then added and the mixture was boiled at 85 °C for 5 min. The product was separated by SDS-PAGE and proteins were transferred onto a PVDF membrane. The membrane was treated with Blocking One® (Nacalai Tesque, Inc.) at 25 °C for 1 h, washed two times with PBS-T containing NaCl (8.0 g/L), KCl (0.2 g/L), $Na_2HPO_4 \cdot H_2O$ (2.9 g/L), KH_2PO_4 (0.2 g/L), and 0.1% (v/v) Tween 20, and incubated overnight with anti-EGFR antibody (4 µL) (sc1005; Santa Cruz Biotechnology, Inc., Santa Cruz, CA, USA) in PBS-T (25 mL) at 25 °C. The membrane was washed three times in PBS-T for 10 min, incubated with HRP-conjugated anti-rabbit IgG antibody (0.5 µL) (NA934, GE Healthcare Ltd.) in PBS-T (25 mL) at 25 °C for 1 h, and washed three times in PBS-T for 10 min. Dimeric and monomeric bands of the EGF receptor were visualized by the Amersham ECL Plus system (GE Healthcare Ltd., Buckinghamshire, UK), and intensities were quantified with a Luminescent Image Analyzer, LAS-4000mini (FUJIFILM Corporation, Tokyo, Japan). Data represent the mean ± standard deviation for at least three independent experiments performed in duplicate.

4.5. EGF receptor autophosphorylation assay

A431 cells in the DMEM supplemented with 10% FBS and 1% penicillin–streptomycin (v/v; 10,000 units/mL and 10,000 µg/mL, respectively) were seeded at 1×10^4 cells per well in 24-well plates and allowed to grow at 37 °C for 4 days in the incubator under 5% CO_2 . After starvation in serum-free medium containing 1 mg/mL of BSA (bovine serum albumin) at 37 °C for 24 h, the cells were treated with the peptide **20** or PBS at 37 °C for 1 h. They were then treated with 100 ng/mL of human EGF (recombinant, R&D Systems, Inc., Minneapolis, MN) at 37 °C for 5 min, put on ice and quickly washed three times with cold PBS. The cells were solubilized on ice for 10 min with a lysis buffer containing 50 mM HEPES (pH 7.4), 1% (v/v) NP-40, 150 mM NaCl, 10% (v/v) glycerol, 1% (v/v) Protease Inhibitor Cocktail (100×) (Nacalai Tesque, Inc.) and 1% (v/v) Phosphatase Inhibitor Cocktail (100×) (Nacalai Tesque, Inc.). To remove the cell debris, the extracts were centrifuged at $14,000 \times g$ for 10 min at 4 °C, and the protein concentrations of the whole-cell lysate were measured with a BCA™ Protein Assay kit (Thermo Fisher Scientific Inc.). The supernatant was diluted with the lysis buffer to 500 µg/mL of protein. An aliquot was mixed with DTT and NuPAGE® LDS Sample Buffer (4×) (Life Technologies Corporation), and the mixture was boiled at 85 °C for 5 min. The product was separated by SDS-PAGE (NuPAGE® 4–12% Bis-Tris Gel, Life Technologies Corporation) and proteins were transferred onto a PVDF membrane. The membrane was treated with Blocking One-P® (Nacalai Tesque, Inc.) at 25 °C for 30 min, washed twice with TBS-T containing tris(hydroxymethyl)aminomethane (2.4 g/L), NaCl (8.0 g/L), and 0.1% (v/v) Tween 20 for 5 min, and incubated overnight with anti-EGFR [pY1068] ABfinity™ Recombinant rabbit monoclonal Antibody-Purified (4 µL) (Life Technologies Corporation) in TBS-T (25 mL) at 25 °C. The membrane was washed three times in TBS-T for 10 min, incubated with HRP-conjugated anti-rabbit IgG antibody (2.5 µL) (NA934, GE Healthcare Ltd.) in TBS-T (25 mL) at 25 °C for 1 h, and washed three times in TBS-T for 10 min. Phosphorylated bands of the EGF receptor were visualized by the Amersham™ ECL Prime system (GE Healthcare Ltd), and intensities were quantified with a Luminescent Image Analyzer, LAS-4000mini. Data represent the mean for two independent experiments performed in duplicate. To determine the receptor amounts loaded in each lane of the SDS-PAGE gel, the blotted membrane was treated with Stripping Solution (Wako Pure Chemical Ind., Ltd, Osaka, Japan) at 25 °C for 10 min, and re-probed with a rabbit polyclonal anti-EGFR antibody (1005) in combination with a peroxidase-linked anti-rabbit IgG secondary antibody (NA934).

4.6. Cell growth assay

A431 cells in the DMEM supplemented with 10% FBS and 1% penicillin–streptomycin (v/v; 10,000 units/mL and 10,000 µg/mL, respectively) were seeded at 5×10^3 cells per well in 96-well plates and allowed to grow at 37 °C for 24 h in the incubator under 5% CO_2 . The cells were treated with distilled water or 10 µM of test peptide and re-incubated at 37 °C for 24 h for three consecutive days. Cell count reagent SF containing WST-8 (10 µL/well) was added to each well and the plate was incubated at 37 °C under 5% CO_2 for 90 min. Absorption values at 450 nm (reference: 655 nm) were measured on a Microplate Reader SH-1000 Lab. Data represent the mean ± standard deviation. Each experiment was performed in six replicate wells and independently repeated three times.

Acknowledgments

This study was supported in part by the 21st Century COE Program and the 'Academic Frontier' Project for Private Universi-

ties of the Ministry of Education, Culture, Sports, Science and Technology (MEXT) of Japan, by a Grant-in-Aid (to K.S.) for Scientific Research from the Japan Society for the Promotion of Science (JSPS), by a research grant from the Naito Foundation (to K. S.), and by a Grant-in-Aid for JSPS Fellows (to T. M.). We are grateful to Ms. K. Oda for FAB mass spectral measurements.

Supplementary data

Supplementary data (HPLC data for the oxidation of **8**, HPLC profiles of test peptides **1–28**, and typical examples of monomeric and dimeric bands of the EGF receptor) associated with this article can be found in the online version, at <http://dx.doi.org/10.1016/j.bmc.2012.08.013>.

References and notes

- Ullrich, A.; Coussens, L.; Hayflick, J. S.; Dull, T. J.; Gray, A.; Tam, A. W.; Lee, J.; Yarden, Y.; Libermann, T. A.; Schlessinger, J.; Downward, J.; Mayes, E. L. V.; Whittle, N.; Waterfield, M. D.; Seeburg, P. H. *Nature* **1984**, *309*, 418.
- Graus-Porta, D.; Beerli, R. R.; Daly, J. M.; Hynes, N. E. *EMBO J.* **1997**, *16*, 1647.
- Hendler, F. J.; Ozanne, B. W. *J. Clin. Invest.* **1984**, *74*, 647.
- Veale, D.; Ashcroft, T.; Marsh, C.; Gibson, G. J.; Harris, A. L. *Br. J. Cancer* **1987**, *55*, 513.
- Sozzi, G.; Miozzo, M.; Tagliabue, E.; Calderone, C.; Lombardi, L.; Pilotti, S.; Pastorino, U.; Pierotti, M. A.; Della Porta, G. *Cancer Res.* **1991**, *51*, 400.
- Rusch, V.; Baselga, J.; Cordon-Cardo, C.; Orazem, J.; Zaman, M.; Hoda, S.; McIntosh, J.; Kurie, J.; Dmitrovsky, E. *Cancer Res.* **1993**, *53*, 2379.
- Ciardiello, F.; Caputo, R.; Bianco, R.; Damiano, V.; Pomatice, G.; De Placido, S.; Bianco, A. R.; Tortora, G. *Clin. Cancer Res.* **2000**, *6*, 2053.
- Anderson, N. G.; Ahmad, T.; Chan, K.; Dobson, R.; Bundred, N. J. *Int. J. Cancer* **2001**, *94*, 774.
- Kawamoto, T.; Sato, J. D.; Le, A.; Polikoff, J.; Sato, G. H.; Mendelsohn, J. *Proc. Natl. Acad. Sci. U.S.A.* **1983**, *80*, 1337.
- Sato, J. D.; Kawamoto, T.; Le, A. D.; Mendelsohn, J.; Polikoff, J.; Sato, G. H. *Mol. Biol. Med.* **1983**, *1*, 511.
- Goldstein, N. I.; Prewett, M.; Zuklys, K.; Rockwell, P.; Mendelsohn, J. *Clin. Cancer Res.* **1995**, *1*, 1311.
- Inoue, A.; Saijo, Y.; Maemondo, M.; Gomi, K.; Tokue, Y.; Kimura, Y.; Ebina, M.; Kikuchi, T.; Moriya, T.; Nukiwa, T. *Lancet* **2003**, *361*, 137.
- Norum, J. *J. Chemother.* **2006**, *18*, 532.
- Starling, N.; Tilden, D.; White, J.; Cunningham, D. *Br. J. Cancer* **2007**, *96*, 206.
- Lemmon, M. A.; Bu, Z.; Ladbury, J. E.; Zhou, M.; Pinchasi, D.; Lax, I.; Engelman, D. M.; Schlessinger, J. *EMBO J.* **1997**, *16*, 281.
- Schlessinger, J. *J. Cell Biol.* **1986**, *103*, 2067.
- Yarden, Y.; Schlessinger, J. *Biochemistry* **1987**, *26*, 1434.
- Yarden, Y.; Schlessinger, J. *Biochemistry* **1987**, *26*, 1443.
- Schlessinger, J. *Cell* **2002**, *110*, 669.
- Carpenter, G.; King, L., Jr.; Cohen, S. J. *Biol. Chem.* **1979**, *254*, 4884.
- Ogiso, H.; Ishitani, R.; Nureki, O.; Fukai, S.; Yamanaka, M.; Kim, J.-H.; Saito, K.; Sakamoto, A.; Inoue, M.; Shirouzu, M.; Yokoyama, S. *Cell* **2002**, *110*, 775.
- Garrett, T. P.; McKern, N. M.; Lou, M.; Elleman, T. C.; Adams, T. E.; Lovrecz, G. O.; Kofler, M.; Jorissen, R. N.; Nice, E. C.; Burgess, A. W.; Ward, C. W. *Mol. Cell* **2003**, *11*, 495.
- Cho, H. S.; Leahy, D. J. *Science* **2002**, *297*, 1330.
- Bouyain, S.; Longo, P. A.; Li, S.; Ferguson, K. M.; Leahy, D. J. *Proc. Natl. Acad. Sci. U.S.A.* **2005**, *102*, 15024.
- Schlessinger, J. *Cell* **2000**, *103*, 211.
- Xu, R.; Povlsen, G. K.; Soroka, V.; Bock, E.; Berezin, V. *Cell Oncol.* **2010**, *32*, 259.
- Yang, R. Y. C.; Yang, K. S.; Pike, L. J.; Marshall, G. R. *Chem. Biol. Drug Des.* **2010**, *76*, 1.
- Mizuguchi, T.; Uchimura, H.; Kakizawa, T.; Kimura, T.; Yokoyama, S.; Kiso, Y.; Saito, K. *Bioorg. Med. Chem. Lett.* **2009**, *19*, 3279.
- Haigler, H.; Ash, J. F.; Singer, S. J.; Cohen, S. *Proc. Natl. Acad. Sci. U.S.A.* **1978**, *75*, 3317.
- Fanger, B. O.; Stephens, J. E.; Staros, J. V. *FASEB J.* **1989**, *3*, 71.
- Staros, J. V. *Biochemistry* **1982**, *21*, 3950.
- Chorev, M. *Acc. Chem. Res.* **1993**, *26*, 266.
- Chorev, M. *Biopolymers (Pept. Sci.)* **2005**, *80*, 67.
- Tatsumi, T.; Awahara, C.; Naka, H.; Aimoto, S.; Konno, H.; Nosaka, K.; Akaji, K. *Bioorg. Med. Chem.* **2010**, *18*, 2720.
- Foy, K. C.; Liu, Z.; Phillips, G.; Miller, M.; Kaumaya, P. T. P. *J. Biol. Chem.* **2011**, *286*, 13626.
- Gaston, F.; Granados, G. C.; Madurga, S.; Rabanal, F.; Lakhdar-Ghazal, F.; Giralt, E.; Bahraoui, E. *ChemMedChem* **2009**, *4*, 570.
- Garrett, T. P. J.; McKern, N. M.; Lou, M.; Elleman, T. C.; Adams, T. E.; Lovrecz, G. O.; Zhu, H.-J.; Walker, F.; Frenkel, M. J.; Hoyne, P. A.; Jorissen, R. N.; Nice, E. C.; Burgess, A. W.; Ward, C. W. *Cell* **2002**, *110*, 763.
- Yamazaki, T.; Zaal, K.; Hailey, D.; Presley, J.; Lippincott-Schwartz, J.; Samelson, L. E. *J. Cell Sci.* **2002**, *115*, 1791.